Int. J. Heat Mass Transfer. Vol. 35, No. 1, pp. 263–267, 1992
Printed in Great Britain

0017–9310/92 $5.00 + 0.00

TECHNICAL NOTE

Buoyancy effect on the laminar forced convection in a horizontal tube with a longitudinal thin plate insert

JUN-DAR CHEN and SHOU-SHING HSIEH†
Department of Mechanical Engineering, National Sun Yat-Sen University, Kaohsiung, Taiwan 80424, Republic of China

(*Received* 3 *July* 1990 *and in final form* 15 *January* 1991)

INTRODUCTION

THE BUOYANCY effect on convective heat transfer in ducts has been extensively examined in the past decade [1, 2]. However, for doubly-connected ducts, only results for concentric tube annuli were obtained in the literature. The fully developed laminar mixed convections in circular annuli of one heated and one adiabatic wall, or of two heated walls were analyzed experimentally [3] and numerically [4]. Nguyen *et al.* [5] studied the mixed convection of water between two isothermal cylinders and found that the axial flow shows a tendency to develop in two or even three jets. The occurrence of density inversion was found to completely modify the lateral flow, but to have little effect on the axial flow. Nieckele and Patankar [6] and Kaviany [7] presented numerical results of mixed convection in concentric tube annuli with axially uniform heating at the inner tube and insulated at the outer tube. An additional assumption of circumferentially uniform wall temperature at the inner tube was made in the study by Nieckele and Patankar [6]. All foregoing studies indicate that the buoyancy-induced secondary flow significantly enhances heat transfer.

As a practically used displaceable device, a longitudinal rectangular plate is often inserted in the tubes of heat exchangers to enhance tubeside heat transfer. The physical configuration is shown in Fig. 1. Laminar forced convection in such tubes and heat transfer enhancement of plate inserts have been studied by the authors [8, 9]. This note presents the buoyancy effect on these characteristics. To place emphasis on determining the influences of the Rayleigh and Prandtl numbers and the inclination of a plate insert to gravity, the aspect ratio (width to height) of a plate insert is fixed at 5 and the radius ratio (of a circumscribed circle of plate insert to the outer circle) at 0.5.

THEORETICAL ANALYSIS

Consider a steady, fully developed laminar flow in a horizontal tube of axially uniform heating and peripherally uniform wall temperature with a plate insert. The fluid properties are assumed constant except for the density, the variation of which is handled by the Boussinesq approximation. Furthermore, the insert is assumed adiabatic to place emphasis on the flow alternation by inserting such plates and the consequent heat transfer alternation. The governing equations which consist of conservation of mass, momentum and energy are made dimensionless using R_0, $(-\mathrm{d}p/\mathrm{d}z)R_0^2/\mu$, α/R_0, $\mu\alpha/R_0^2$, and $q''_{\mathrm{in}}R_0/k$ to scale length, axial velocity (W), lateral velocities (U, V), lateral pressure (P) and relative temperature (T) with respect to constant outer wall temperature [9]. Here $\mathrm{d}p/\mathrm{d}z$ is the axial pressure gradient, μ the dynamic viscosity, α the thermal diffusivity, and k the conductivity.

† Author to whom correspondence should be addressed.

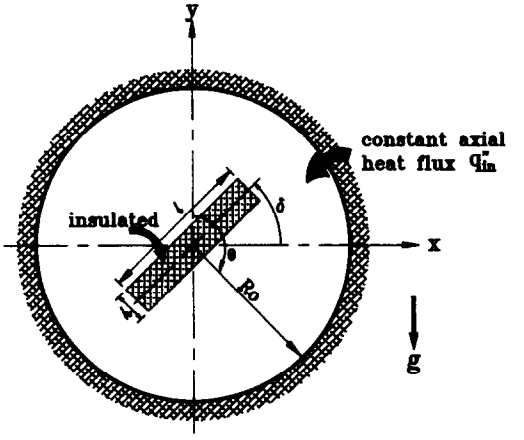

FIG. 1. A noncircular annular duct.

To tackle the irregular flow configuration, the dimensionless governing equations are formulated in a boundary-fitted coordinate system (BFCS) in conservative form and are cast in generalized form as

$$\frac{\partial}{\partial\xi}(U_\xi\phi)+\frac{\partial}{\partial\eta}(U_\eta\phi)=\frac{\partial}{\partial\xi}\left[\frac{\Gamma}{J}\left(\alpha\frac{\partial\phi}{\partial\xi}-\beta\frac{\partial\phi}{\partial\eta}\right)\right]+\frac{\partial}{\partial\eta}\left[\frac{\Gamma}{J}\left(\gamma\frac{\partial\phi}{\partial\eta}-\beta\frac{\partial\phi}{\partial\xi}\right)\right]+S(\xi,\eta) \quad (1)$$

where α, β, γ and J are coefficients of the transform, Γ the diffusion coefficient and S the source term of the generalized variable ϕ. Table 1 shows the expressions of Γ and S for each variable in which A_f and P_0 are dimensionless flow area and tube perimeter, respectively, W_m the dimensionless cross-sectional mean axial velocity, D_h the dimensionless hydraulic diameter [9], Ra the Rayleigh number ($=\beta g q''_{\mathrm{in}} d_h^4/k\nu\alpha$), Pr the Prandtl number ($=\nu/\alpha$), β the coefficient of thermal expansion, g the gravitational acceleration, and d_h the dimensional hydraulic diameter. U_ξ and U_η are known as contravariant velocities in the ξ- and η-directions, which are related to U and V via $U_\xi = UY_\eta - VX_\eta$ and $U_\eta = VX_\xi - UY_\xi$ [10]. As for boundary conditions, each variable vanishes at all boundaries except temperature at the inner wall where its normal gradient vanishes [9].

A nonorthogonal 73×36 grid with nodes equi-spaced along, and grid lines more closely packed near the walls, is used for computation [9]. Equation (1) is discretized by the finite-volume discretized method in a staggered grid system. The extended SIMPLE algorithm in BFCS [10] is used for the pressure–velocity coupling and the power-law scheme [11] is used to approximate the convection term. The dis-

Table 1. Coefficients of the governing equations

Equation	ϕ	Γ	$S(\xi,\eta)$
Continuity	1	1	0
X-Momentum	U	Pr	$Pr\,Y_\xi P_\eta - Pr\,Y_\eta P_\xi$
Y-Momentum	V	Pr	$(J\,Ra\,Pr\,T)/D_h^4 - Pr\,X_\xi P_\eta + Pr\,X_\eta P_\xi$
Z-Momentum	W	Pr	$J\,Pr$
Energy	T	1	$-JWP_0/W_m A_f$

cretized equation of all variables are iteratively solved in a sequential manner by line-by-line procedure. The iterative procedure is terminated when $|(\phi^{n+1}-\phi^n)/\phi^{n+1}| < 10^{-6}$ for $\phi = T$ and W at each node, then the friction factor–Reynolds number product, $f\,Re$, local and averaged Nusselt numbers of the outer wall, Nu and Nu_m, defined in ref. [9], are calculated by the converged solutions. To facilitate the presentation of the secondary flow pattern, a dimensionless cross-sectional stream function ψ is so defined as to be calculated from the velocity components by

$$\psi = \int_{\eta_i}^{\eta} U_\xi \, d\eta$$

with $\psi = 0$ at $\eta = \eta_i$ (inner wall).

RESULTS AND DISCUSSION

The numerical solutions are obtained for values of Ra ranging from 10^3 to 10^6 with two Prandtl numbers of 0.7 and 7.0, and inclined angle (δ) of the insert of 0°, 45° and 90°. To verify the present solution procedure, computations are first performed for mixed convection in concentric tube annuli with axially uniform heating at the inner tube and insulated at the outer tube, corresponding to the case of Nieckele and Patankar [6] for RR (radius ratio of inner to outer tubes) = 0.5. Figure 2 presents the ratio of mixed convection to forced convection for Nu_m and that for $f\,Re$. These ratios obtained by the present study are in good agreement with those obtained by Nieckele and Patankar [6]. Furthermore, the grid dependence of the results of the present study is examined by a finer 97×44 grid in some cases of the problem studied. The variations of Nu_m and $f\,Re$ are less than 1% at high Rayleigh number and are much less at low Rayleigh number.

The cross-sectional temperature and flow patterns are shown in Fig. 3 by equi-spaced isotherms and streamlines for some cases. For symmetry, the isotherms are plotted in the left half and the streamlines in the right half of each annulus, except for the case of $\delta = 45°$ where streamlines and isotherms are separately plotted in the whole annulus. The values of T_{min} (a measure of the extent of fluid mixing) and ψ_{max} and/or ψ_{min} (measures of the strengths of the vortexes) are listed below the annuli. Note that the stream function is positive in a counter-clockwise rotating vortex and negative in a clockwise one. The dot in these figures denotes the rotating center of a vortex where ψ_{max} or ψ_{min}, depending on its rotating direction, is located.

For an insert of $\delta = 0°$, the left part of Fig. 3 shows the effect of Prandtl number for various Rayleigh numbers. By the specified thermal boundary conditions, the isotherms are closely packed near the bottom zone and become more obvious at larger Ra. The thermal boundary layer is well developed along the tube. At $Ra = 10^4$, weak secondary flow is induced and exhibits a structure of two subvortexes above and beneath the insert within a main vortex. The lower subvortex is stronger than the upper one. All these vortexes rotate in the same direction. The temperature pattern of pure forced convection [8] is slightly affected. When the Rayleigh number increases, the subvortexes vanish, the main vortex becomes stronger, and the rotating center of the main vortex shifts upwards. Hot fluids with stratified temperature distribution exist above the insert. Furthermore, fluid heated at the bottom zone releases its thermal energy during circulating motion, thus becoming cold below the insert, where the phenomenon of temperature inversion occurs. Similar flow and temperature patterns are observed for both values of Pr, with the fluid of higher Pr having a stronger secondary flow at the same Ra [6]. Thus, the results of $Pr = 0.7$ will be sufficient for the analysis hereafter. As shown in the right part of Fig. 3, tilting the insert makes the suppressing force of the insert different in the left and right halves of the cross section. The left vortex is stronger than or at least equal to the right one. The cold fluid region shifts somewhat towards

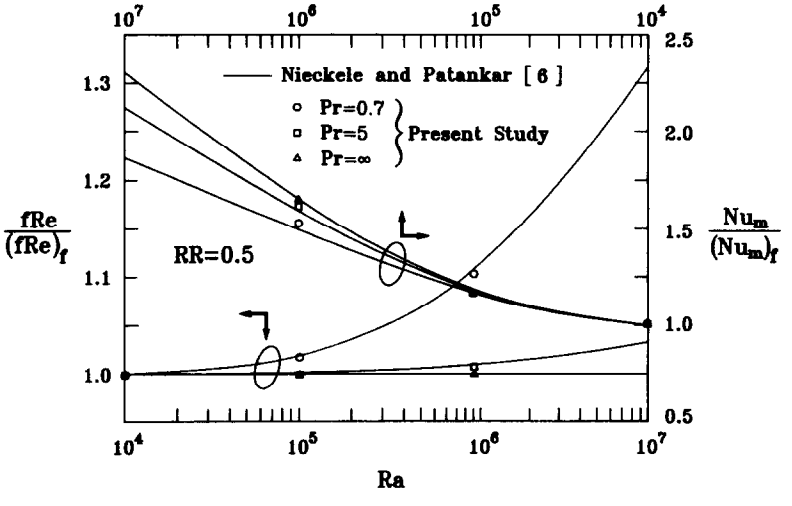

FIG. 2. $f\,Re$ and Nu_m ratios of mixed to forced convection in a horizontal concentric tube annulus.

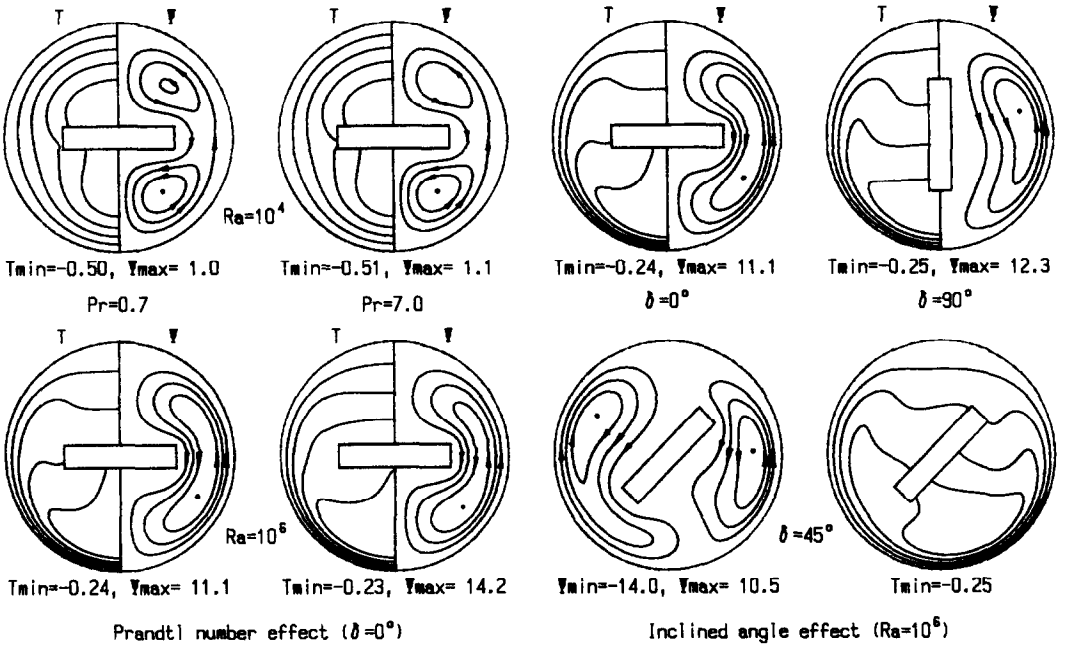

FIG. 3. Cross-sectional flow and temperature patterns of some cases of the problem studied.

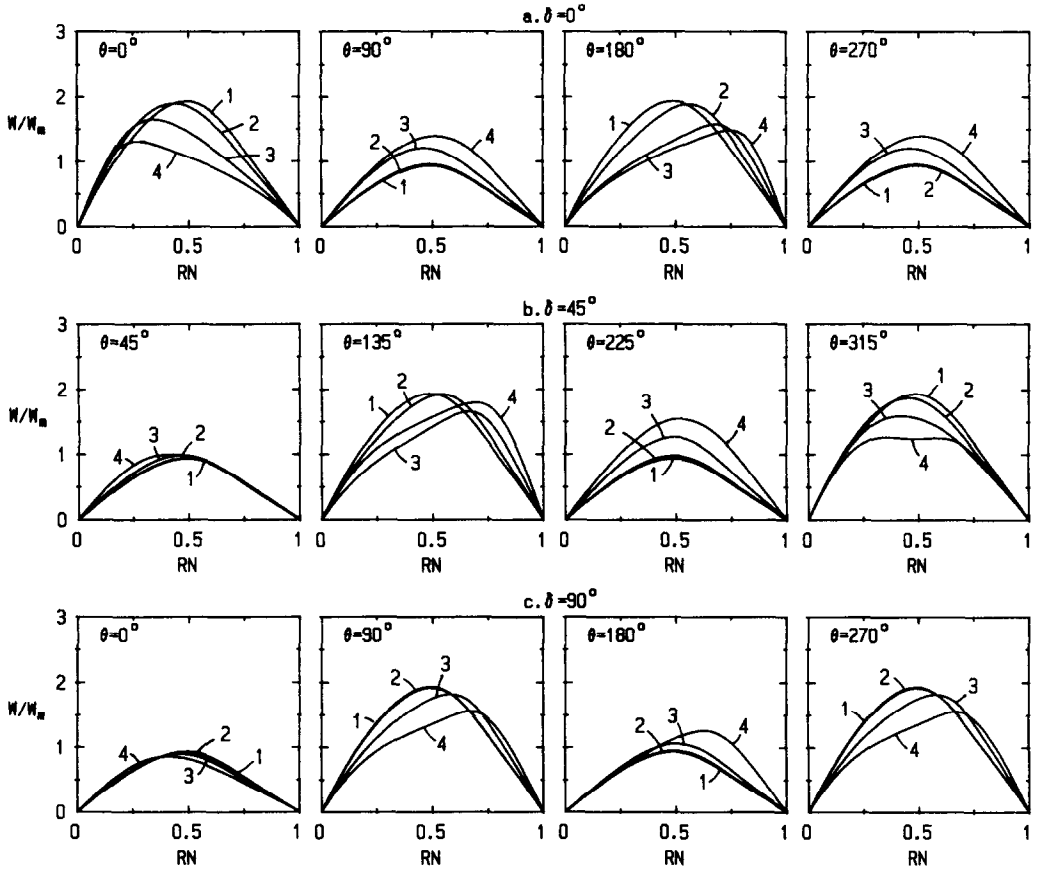

FIG. 4. Effects of Rayleigh number on the axial velocity profile: 1, $Ra = 0$; 2, $Ra = 10^4$; 3, $Ra = 10^5$; 4, $Ra = 10^6$.

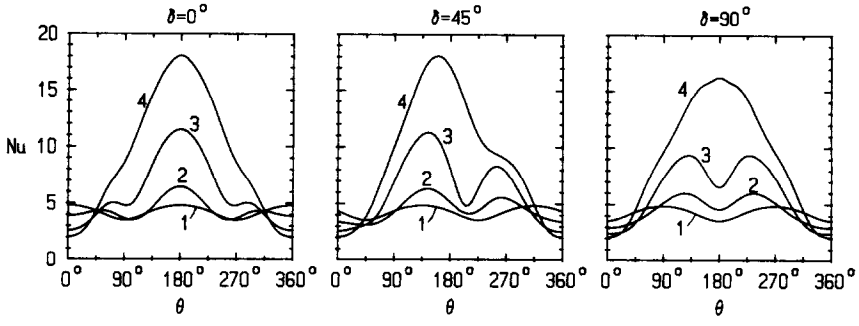

FIG. 5. Effects of Rayleigh number on the local Nusselt number: 1, $Ra = 0$; 2, $Ra = 10^4$; 3, $Ra = 10^5$; 4, $Ra = 10^6$.

the right. In the case of $\delta = 90°$, temperature stratification exists in the core region of the tube, which exists similarly in an axially uniformly heated horizontal bare tube.

Figure 4 shows the influence of secondary flow on the axial velocity profiles at angular locations through the midpoints of the plate sides. The RN denotes the normalized (with respect to gap clearance) radial distance in each angular location with $RN = 0$ for the insert and $RN = 1$ for the tube. Despite the inclined angle of the insert, secondary flow increases axial velocity at a small clearance gap but decreases at a larger clearance gap. The peak of axial velocity at the upper gap shifts towards the inner wall but that at the lower gap shifts towards the outer tube. For a plate with $\delta = 45°$, axial velocity profiles in the right vortex are slightly affected due to its lower strength. In contrast, the left strong vortex greatly affects the axial velocity profiles in the left part of the cross section.

The angular variations of the local Nusselt number of the tube are shown in Fig. 5 for three values of δ. Although increasing Ra upgrades Nu in most regions, values of Nu near the top ($\theta = 0$ or 360°) decrease by the secondary flow. In general, since most fluid below the insert is cold, a large temperature gradient and, in turn, a high local Nusselt number occurs near the bottom ($\theta = 180°$). Table 2 summarizes the values of Nu_m and $f\,Re$ of the present study. For both values of Pr, it is found that while the $f\,Re$ factor decreases with increasing δ for each Ra, the dependence of Nu_m on δ varies with Ra. However, the discrepancies between values of Nu_m of different δ for the same Ra are so small as to be neglected for practical purposes.

Close inspection of Table 2 reveals that secondary flow augments heat transfer and increases the pumping power simultaneously. Due to its high viscosity, fluid of high Pr has a greater alleviative buoyancy effect on $f\,Re$ than that of low Pr. However, for the same Ra, increasing the value of Pr decreases Nu_m in most cases studied. Although contrary to the common observation, this finding has also been observed by Kaviany [7] for $Ra \leqslant 10^6$. Since the common observation reappears at higher Ra in the Kaviany study, it is therefore inferred that increasing Pr will increase Nu_m only when Ra is larger than a certain value, which is problem dependent. However, the difference between the values of Nu_m of various Pr is small and can be neglected for practical purposes. These values of Nu_m are correlated via a least-square method in the form of $Nu_m = 1.025Ra^{0.1586}$ which is valid for $0.7 \leqslant Pr \leqslant 7.0$ and $10^4 \leqslant Ra \leqslant 10^6$ with a maximum error of $\pm 6.71\%$.

CONCLUSION

This paper presents a numerical study for the buoyancy effect on the fully developed laminar forced convection in an axially uniformly heated tube with a concentric adiabatic plate insert. The computations are carried out for a range of Rayleigh numbers, Prandtl numbers and the inclined angles of the insert.

Increasing the Rayleigh number increases the strength of the secondary flow and collects colder fluid below the plate. Meanwhile, fluid temperature stratification occurs above the plate. The effect of Prandtl number on the flow and temperature patterns becomes obvious as the Rayleigh number increases. Tilting the plate insert results in the left vortex stronger than or at least equal to that of the right one. The onset of secondary flow augments the heat transfer and increases the pumping power. While increasing the Prandtl number or tilting the insert decreases the $f\,Re$ factor for the same Rayleigh number, the value of Nu_m is only slightly affected by these changes. A correlation equation for values of Nu_m is also recommended.

REFERENCES

1. H. V. Mahaney, F. P. Incropera and S. Ramadhyani, Development of laminar mixed convection flow in a horizontal rectangular duct with uniform bottom heating, *Numer. Heat Transfer* **12**, 137–155 (1987).
2. F. C. Chou and G. J. Hwang, Numerical analysis of the

Table 2. Overall Nusselt number and $f\,Re$ factor

		$Ra = 10^3$		$Ra = 10^4$		$Ra = 10^5$		$Ra = 10^6$	
δ	Pr	$f\,Re$	Nu_m	$f\,Re$	Nu_m	$f\,Re$	Nu_m	$f\,Re$	Nu_m
0°	0.7	21.63	4.276	21.97	4.466	24.74	6.072	29.69	9.416
	7.0	21.63	4.275	21.63	4.429	21.73	5.962	22.29	9.405
45°	0.7	21.63	4.277	21.87	4.524	24.09	6.197	28.62	9.314
	7.0	21.63	4.276	21.63	4.491	21.70	6.117	22.17	9.315
90°	0.7	21.63	4.278	21.73	4.564	23.11	6.126	27.80	9.351
	7.0	21.63	4.278	21.63	4.556	21.66	6.139	22.02	9.288

Graetz problem with natural convection in a uniformly heated horizontal tube, *Int. J. Heat Mass Transfer* **31,** 1299–1308 (1988).
3. N. Hattori and S. Kotake, Combined free and forced convection heat transfer for fully developed flow in horizontal tubes (experiments), *Bull. JSME* **8,** 861–868 (1978).
4. N. Hattori, Combined free and forced convection heat transfer for fully developed laminar flow in horizontal concentric annuli (numerical analysis), *Heat Transfer—Jap. Res.* **8,** 27–48 (1979).
5. T. H. Nguyen, P. Vasseur, L. Robillard and B. Chandrasekhar, Combined free and forced convection of water between horizontal concentric cylinders, *J. Heat Transfer* **105,** 498–504 (1983).
6. A. O. Nieckele and S. V. Patankar, Laminar mixed convection in a concentric annulus with horizontal axis, *J. Heat Transfer* **107,** 902–909 (1985).
7. M. Kaviany, Laminar combined convection in a horizontal annulus subject to constant heat flux inner wall and adiabatic outer wall, *J. Heat Transfer* **108,** 392–397 (1986).
8. J. D. Chen and S. S. Hsieh, Laminar forced convection in circular tube inserted with a longitudinal rectangular plate, *J. Thermophys. Heat Transfer* (in press).
9. J. D. Chen and S. S. Hsieh, Assessment study of longitudinal rectangular plate inserts as tubeside heat transfer augmentative devices, *Int. J. Heat Mass Transfer* **34,** 2545–2553 (1991).
10. W. Shyy, S. S. Tong and S. M. Correa, Numerical recirculating flow calculation using a body-fitted coordinate system, *Numer. Heat Transfer* **8,** 99–113 (1985).
11. S. V. Patankar, *Numerical Heat Transfer and Fluid Flow*, 1st Edn. Hemisphere, New York (1980).